ACS Photonics

pubs.acs.org/journal/apchd5

Article

Dynamically Tunable Terahertz Emission Enabled by Anomalous Optical Phonon Responses in Lead Telluride

Burak Guzelturk,* Mariano Trigo, Olivier Delaire, David A. Reis, and Aaron M. Lindenberg*

Cite This: https://doi.org/10.1021/acsphotonics.1c01291

Read Online

ACCESS | Metrics & More | Article Recommendations | Supporting Information

ABSTRACT: Lead telluride (PbTe), a narrow bandgap semiconductor commonly used in infrared detectors, exhibits anomalous vibrational and structural properties, making it appealing for thermoelectrics. Despite significant fundamental interest in the microscopic origins of its unusual vibrational properties, the optical functionalities stemming from phonons and electron−phonon coupling in PbTe have not been closely investigated. This paper reports measurements of terahertz (THz) radiation from a PbTe single crystal following ultrafast optical excitation and investigates IR-active phonon responses as a function of excitation fluence and temperature. We uncover a spectrally tunable THz emission peak enabled by an epsilon-near-zero response of the coupled plasmon−longitudinal optical phonon mode that can be dynamically shifted via tuning photocarrier density. Spectral tunability ($\Delta\omega/\omega$ = 25%) is significant and beyond what has been achieved by any other THz emitter. In addition, the emitted THz fields reveal signatures of a zone center transverse optical phonon anomaly and unveil a new mode at 0.3 THz that diminishes in amplitude under increasing photocarrier density. Temperature-dependent measurements suggest that the transverse-like modes at 1 and 1.5 THz are possibly of different origins. These results indicate that the unusual phononic properties in PbTe are tunable via photoexcitation and enable new optical functionalities in THz applications, such as spectrally tunable emitters and all-optical modulators.

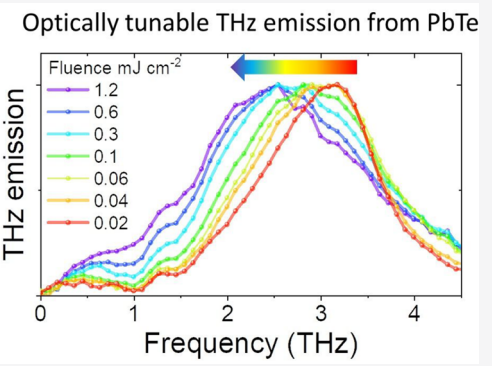

KEYWORDS: *terahertz emission, lead telluride, optical phonons, epsilon-near-zero, plasma coupling*

Lead telluride (PbTe), which crystallizes in the cubic, rocksalt structure, exhibits unusual vibrational and electronic properties, leading to an ultralow lattice thermal conductivity and positive temperature coefficient for the bandgap[1−4] that have led to its utilization as a high performance thermoelectric material.[5] Underpinning these properties, early reports pointed out the importance of structural instabilities and soft transverse optical phonon mode responses associated with incipient ferroelectric behavior.[2,6] More recently, inelastic neutron scattering measurements elucidated phonon anomalies in PbTe,[7−9] including avoided crossings between optical and acoustic phonon branches and highly anharmonic modes.[7] Particularly, the zone-center transverse optical phonon has been shown to exhibit a temperature-dependent double-peak feature,[7,9] which is unexpected for a rocksalt crystal due to its cubic symmetry. In addition, a waterfall-like dispersion of the transverse mode extending to lower energies has been observed,[7] which resemble those in relaxor-type ferroelectrics arising from polar nanodomains.[10,11] Indeed, total[8] and diffuse[12] scattering measurements have suggested the presence of correlated local structural fluctuations in PbTe at room temperature. The discovery of these unusual vibrational and structural properties in PbTe has led to significant research efforts to uncover the underlying microscopic mechanisms.[13−20] Nevertheless, little is known concerning the optical responses of phonons in PbTe and their functionalities toward THz applications.

Optical phonons in PbTe lie in a spectral range of 1−3 THz[2,21] and display a giant splitting between longitudinal (LO) and transverse optical (TO) phonon modes. In a polar material, the LO−TO splitting intrinsically arises from the bond polarizability of the material, expressed by the Born effective charge (Z_s), where the splitting scales with Z_s^2. PbTe possesses a very large Z_s of 6,[22] whereas in conventional polar semiconductors (e.g., GaAs), Z_s is ∼2. A large LO−TO splitting also implies a significant contrast between optical (ε_∞) and static (ε_{static}) dielectric coefficients, as one can infer from the Lydanne−Sachs−Teller relationship $\frac{\omega_{LO}^2}{\omega_{TO}^2} = \frac{\varepsilon_{static}}{\varepsilon_\infty}$ where ω_{LO} and ω_{TO} are the LO and TO phonon frequencies, respectively. ε_{static} and ε_∞ in PbTe[2] were measured to be ∼400 and 32 at room temperature, respectively, resulting in a $\frac{\varepsilon_{static}}{\varepsilon_\infty}$

Received: August 24, 2021

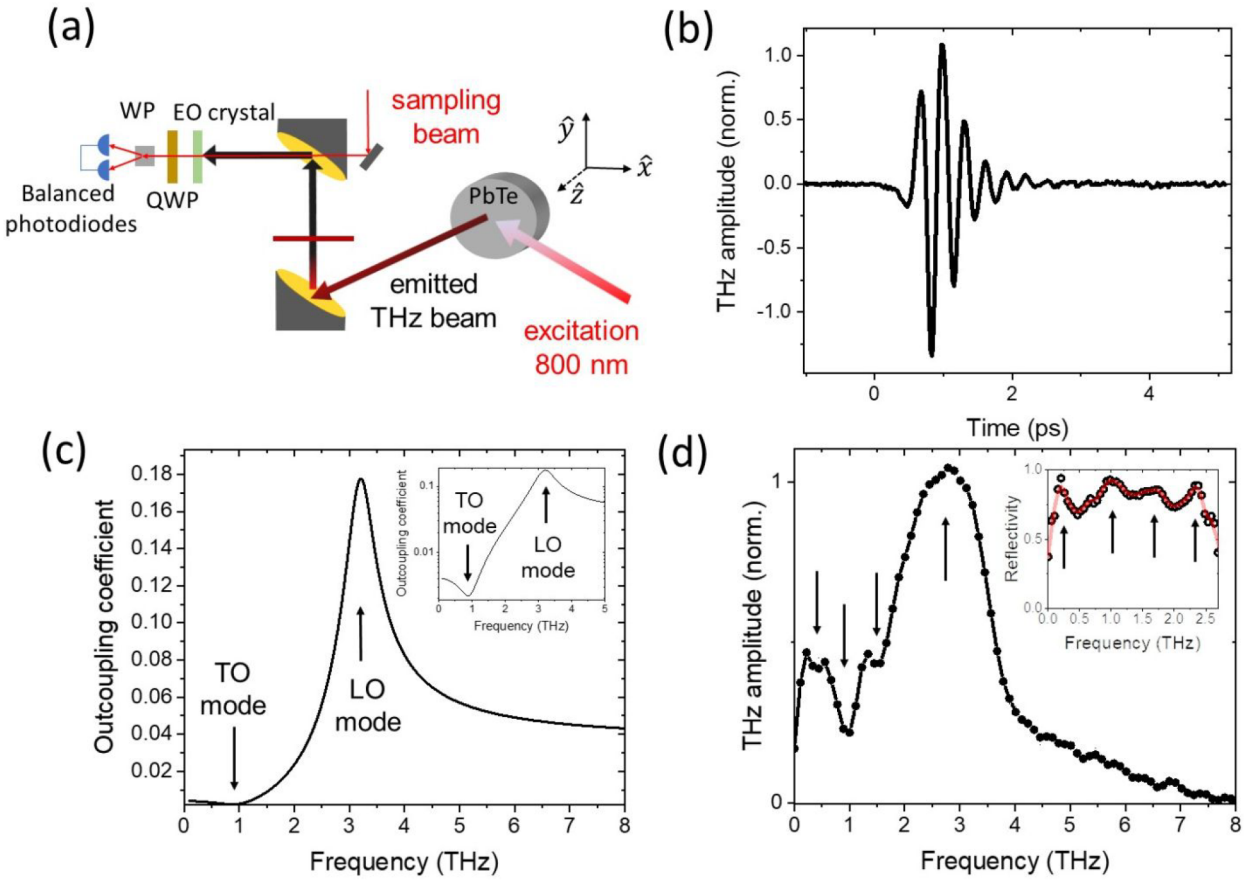

Figure 1. (a) THz emission setup in a reflection geometry. The sample is excited with a 800 nm, 50 fs, 5 MHz repetition rate laser. WP, QWP, and EO crystal denotes Wollaston prism, quarter wave plate, and electro-optic crystal, respectively. (b) Emitted THz field amplitude from PbTe in the time domain measured under an excitation fluence of 23 μJ cm^{-2}. (c) Calculated outcoupling coefficient from PbTe exhibiting dip and peak due to transverse optical (TO) and longitudinal optical (LO) phonon modes, respectively. The inset shows the outcoupling coefficient in log scale for a zoomed in region. (d) Emitted THz spectrum under low photo excitation density. The inset shows the THz reflectivity from PbTe crystal surface measured in 0−2.5 THz range. Peaks in the reflectivity indicates the spectral location of transverse mode resonances.

ratio of ∼12. The same ratio is ∼1.5 for prototypical polar semiconductors, which also have much smaller dielectric coefficients (ε < 20). PbTe with large dielectric coefficients and spectrally distinct LO and TO modes is expected to express a broadband and prominent Reststrahlen band in the THz window. Reststrahlen bands emerge in polar materials where the optical reflectivity varies from very high to very low in a narrow spectral window as frequency is swept from that of the TO to LO phonons.[23] Highly pronounced and broadband Reststrahlen bands in the THz range could enable new ways to manipulate electromagnetic fields, which has been particularly challenging due to material and component limitations in this spectral range. Early work on PbTe using static reflectivity measurements hinted at a broad Restrahlen response,[21,24] yet associated phonon modes were not well-resolved due to limited measurement bandwidths. Later, Tani et al. showed that PbTe can emit THz radiation following photoexcitation,[25] yet optical phonon signatures could not be distinguished.

Herein, we report broadband spectroscopic measurements of THz emission and reflectivity on a high quality PbTe single crystal.[13] While the emitted THz field strength is comparable to those emitted by the conventional surface THz emitters, such as InAs and InSb,[26] the THz emission from PbTe shows an impressive spectral tunability. Under low photoexcitation density, we find that the emission peak occurs at 3.2 THz stemming from strongly outcoupled THz emission at the LO phonon resonance, occurring at the zero crossing of the dielectric constant. As the photoexcitation density is increased, the THz emission peak strongly red-shifts to 2.4 THz. This spectral shift can be explained by the coupling of a highly damped photoexcited carrier plasma with the LO mode which effectively shifts the epsilon-near-zero response. The emitted THz spectrum also encodes the signatures of the TO phonons, displaying the previously reported double peak feature at 1 and 1.5 THz.[7,9] The temperature-dependent spectral response of these two modes indicates that their microscopic origins are possibly different. Importantly, we unveil a new low-energy feature at ∼0.3 THz, which was not resolved previously. The amplitude of the low-energy mode reversibly vanishes under increasing photocarrier density, hence, opening up a new way to optically modulate low-frequency THz fields.

RESULTS AND DISCUSSION

Upon femtosecond laser excitation with a photon energy of 1.5 eV, a pulse width of 50 fs, and a repetition rate of 5.1 MHz, we observe coherent THz radiation emitted from a PbTe crystal. The sample is excited in a reflection mode (see Figure 1a), and the emitted THz field amplitude and phase are detected by free-space electro-optic sampling.[27] Figure 1b shows an exemplary case of the measured THz field in the time domain,

https://doi.org/10.1021/acsphotonics.1c01291
ACS Photonics XXXX, XXX, XXX−XXX

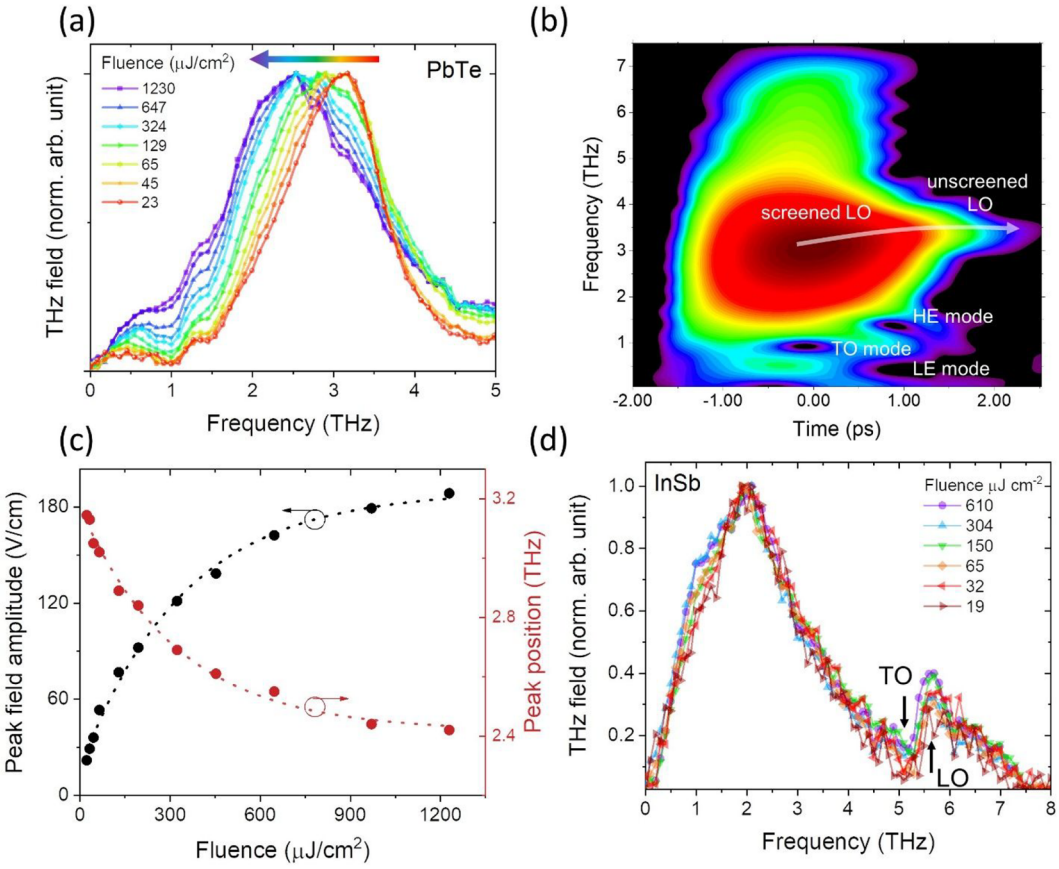

Figure 2. (a) Emitted THz spectra measured in PbTe under increasing excitation fluence. (b) Short-time Fourier transform analysis of the THz emission showing time-frequency response of the TO and LO phonon modes. (c) Emitted THz peak position and peak amplitude as a function of excitation fluence. (d) Emitted THz spectra measured in InSb under increasing excitation fluence. Practically, there is almost no spectral tunability by photodoping.

which displays multicycle oscillations related to the optical phonon contributions, as will be discussed below. To investigate the THz emission mechanism, we first characterize the polarization state of the emitted THz field,[28] which is found to be polarized in the reflection plane, that is, p-polarized (see Figure S1), which holds true for any azimuthal orientation of the sample (Figure S2). These observations imply that the mechanism underlying THz radiation is a transient current flowing parallel to the surface normal direction (parallel to $\hat{z}$, as shown in Figure 1a). Therefore, THz emission in PbTe originates from an ultrafast charge separation along the surface normal direction. Ultrafast charge separation at semiconductor surfaces has been reported before, which may occur either via photo-Dember effect,[26] originating from a difference in the diffusivity of charge carriers, or via surface surge currents due to surface band bending.[29] In addition, insensitivity of the THz emission to the excitation laser polarization (accounting for changes in the reflectivity of the pump laser) and the azimuthal rotation of the sample (Figures S2 and S3) indicates that nonlinear THz emission mechanisms, such as optical rectification, are unlikely to explain the emission mechanism.

The emitted THz spectrum encodes signatures of IR-active optical phonon modes of a material. These signatures are independent of the charge separation mechanism giving rise to the THz emission.[30,31] TO modes show up as spectral dips due to large dielectric coefficients and dielectric loss associated with the TO mode, which minimize the outcoupling efficiency of the radiated THz fields.[32,33] On the other hand, LO modes show up as peaks[33,34] as LO phonons naturally exhibit an epsilon-near-zero (ENZ) response, thus, maximizing the outcoupling at the LO mode resonance.[35] Figure 1c shows the outcoupling coefficient[36] for THz emission calculated using a first-order complex dielectric function, which does not consider TO phonon anomalies in PbTe (see Figure S4).[21] Figure 1c shows that the outcoupling is maximized at ~3.3 THz around the bare LO phonon mode, whereas it is minimized at 1 THz at the TO mode. Having established the expected modifications in the emitted spectrum due to different phonon modes, we now interpret the experimentally measured spectrum in Figure 1d. As labeled in this figure, the main spectral features are dips at 0.3, 1, and 1.5 THz and a peak around 3 THz. While the peak arises from the LO mode, as expected from the maximized outcoupling coefficient (Figure 1c), the dip features are associated with TO-like modes. The origin of the multiple dips is related to the anomalous behavior of the TO phonons previously indicated by inelastic neutron scattering measurements[7,9] and with prior theory,[16−18,20] but here resolved at significantly better frequency resolution. Dip features in Figure 1d are also corroborated by a static THz reflectivity measurement (inset of Figure 1d), where the response is reversed in reflection measurements, hence, the TO-like modes appear as peaks rather than dips.[23] Therefore, THz emission and reflectivity

https://doi.org/10.1021/acsphotonics.1c01291
ACS Photonics XXXX, XXX, XXX−XXX

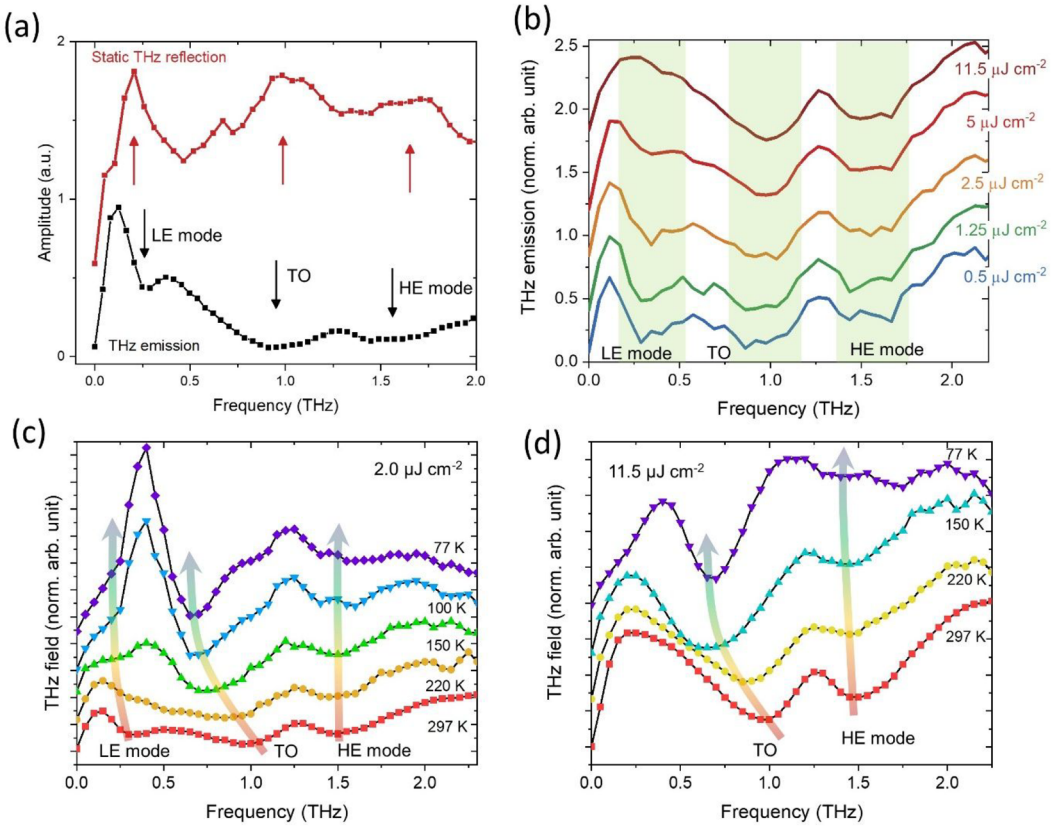

Figure 3. (a) THz emission spectrum optimized for low energy region (0−2.5 THz) to unveil transverse optical (TO) phonon responses. Dip features in the THz emission spectrum and peak features in the static THz reflectivity both consistently show the spectral positions of the TO phonon resonances. (b) Excitation fluence-dependent THz emission spectrum around the TO phonon range. (c, d) Temperature-dependent THz emission spectrum in the TO phonon range. Excitation fluence is 2.0 μJ cm^{-2} in (c) and 11.5 μJ cm^{-2} in (d).

both indicate the presence of multiple low energy modes in PbTe, which will be discussed below.

We now investigate the effect of photoexcited carrier density on the emitted THz fields. Figure 2a shows the normalized emitted spectra measured under increasing excitation fluence. The THz emission peak shifts to lower energy as the excitation density is increased. This observation indicates that the ENZ response is spectrally tunable in PbTe by changing the photocarrier density. The red-shift of the peak is rather strong and the direction of the shift is surprising. In polar semiconductors, free carriers can screen the long-range electric fields associated with LO phonons via carrier plasma oscillations.[37] Conventionally, LO phonon−plasma coupling results in two hybrid modes at a higher and a lower energy,[35] which both blue-shift under increasing carrier density. Contrary to this, we observe a red-shift of the THz emission peak. However, this conventional LO phonon−plasma coupling picture is valid when the plasma is not heavily damped. In the case of a heavily damped plasma, carrier screening can induce a mode that would red-shift from the bare LO mode toward the TO mode as the carrier density is increased.[38] Therefore, the red-shift of the emission peak can be possibly explained by coupling of the LO mode with an overdamped carrier plasma. We calculate the frequency of the screened LO mode by considering the complex dielectric function modified in the presence of a highly damped plasma (Figure S5), which shows that the ENZ mode can be red-shifted by an amount roughly consistent with experimental observations. A separate mechanism that may play a role in the red-shift of the LO mode is the screening of Born-effective charge via free carriers. However, this mechanism is less likely to dominate, as indicated by recent theoretical work, where the Born-effective charge is found to be unscreened even in highly doped semiconductors.[39]

To monitor the temporal evolution of the spectral features in the emitted THz spectrum, we perform a time-frequency analysis of the THz spectrum (see Figure 2b and Methods). The THz peak initially emerges at 3 THz, which is the coupled LO − damped plasma mode, or the screened LO mode. After ∼1 ps, the THz peak shifts to 3.4 THz and stays there, which corresponds to the unscreened bare LO phonon resonance.[2] This indicates that the plasma−LO coupling is dynamic, and the coupling goes down after 1 ps as the plasma is rapidly damped out. Therefore, this allows ultrafast, subpicosecond, tunability of the THz properties in PbTe. Figure 2c shows the peak amplitude and position as a function of excitation fluence, which both evidence a saturation behavior. This indicates that the efficiency of the ultrafast charge separation is reduced under high excitation fluence. This observation can be corroborated by increased carrier−carrier and intervalley scattering in the high carrier density regime, leading to stronger damping and lowered nonequilibrium carrier mobility.[40] Increased damping is further evidenced by shorter-lived oscillations in the radiated field under increased excitation density (see Figure S6). Saturation of the peak shift also implies that the screening efficiency of the LO phonon by plasma coupling is reduced as the carrier−carrier scattering is enhanced. The maximum THz peak field strength is estimated

https://doi.org/10.1021/acsphotonics.1c01291
ACS Photonics XXXX, XXX, XXX−XXX

to be 188 V/cm under an excitation fluence of 1.2 mJ cm^{-2}. As compared to other prototypical surface THz emitters based on III−V semiconductors, the measured field strength in PbTe is on par.[41]

The THz emission peak shifts from 3.2 to 2.4 THz (Figure 2c) as the excitation fluence is increased from 0.02 to 1.2 mJ cm^{-2}, hence, changing the degree of photodoping. Such tunability represents a substantial modulation efficiency of $\frac{\Delta\omega}{\omega} = 25\%$. In conventional THz emitters, such as GaAs and InSb, an optically controlled spectral tunability has not been reported to date. For example, Figure 2d shows normalized THz emission spectra measured from an InSb single crystal under a similar excitation fluence range. The TO and LO phonon modes are labeled at 5.4 and 5.7 THz, respectively. The spectral tunability is practically nonexistent in InSb (Figure 2d). Previously, a few reports using transient reflectivity measurements showed spectral tunability of coherent LO phonons.[30] In GaAs, modulation efficiency was found to be 5%.[38] This is expected as the maximum tunability range is limited to 8% since the LO and TO modes are at 8.7 and 8.1 THz, respectively. This indicates that PbTe provides a significantly enhanced tunability efficiency and bandwidth, which indeed covers most of the THz band in the 1−3 THz range. To further understand the function−property relationship regarding the spectral tunability, we also performed THz emission measurements in another IV−VI semiconductor, SnSe, which exhibits larger polarizability as compared to common III−V semiconductors, yet still smaller than that of PbTe. The TO and LO modes are at 4.3 and 5.9 THz with a theoretical maximum tunability of 27%. The THz peaks associated with the ENZ mode red-shift from 5.8 to 5.0 THz as the excitation density is increased in a similar fluence range (Figure S7). Therefore, SnSe achieves a tunability efficiency of 14%. Although the tunability in SnSe is smaller than that of PbTe, this observation points to the fact that IV−VI based semiconductors with larger polarizability, hencelarger LO-TO splitting are particularly promising as optically controlled tunable THz emitters. Overall, PbTe with large LO-TO splitting arising from its intrinsically large polarizability bestows it with a high degree of tunability of the ENZ response via screening of the LO mode by photoexcited carrier plasma. This highlights the potential of PbTe as a spectrally tunable THz material for various THz photonic applications.[42,43]

To investigate the TO-like phonon responses at lower frequencies (0−2 THz), we boost the signal intensity in this range by switching to a ZnTe electro-optic crystal which has a much higher sensitivity in this range. Also, the excitation spot size on the sample is enlarged to minimize the high pass filtering effect of the first parabolic mirror which collimates the emitted THz waves from the sample. With these modifications, we resolve the dip features on the lower energy side with improved signal-to-noise. Figure 3a shows the emitted THz spectrum, clearly showing dip features at 0.3, 1, and 1.5 THz. Static THz reflectivity measurement (Figure 3a) also agrees with the presence of these three modes. Prior experimental work and theoretical calculations have estimated the frequency of the bare TO phonon mode in PbTe at room temperature to be ∼1 THz.[2,21] Therefore, the feature at 1 THz is labeled here as the bare TO mode. Features at 0.3 and 1.5 THz are labeled as low energy (LE) and high energy (HE) modes since their microscopic origins are not clear. The TO and HE modes, at 1 and 1.5 THz, respectively, have been previously observed by inelastic neutron measurements,[7] while the LE mode at 0.3 THz (∼1 meV) is resolved here for the first time, as it was not in the energy range of prior inelastic neutron scattering measurements due to their low energy cutoff (∼2 meV). Thus, our approach enables higher resolution probing of the low frequency phonon modes in PbTe but, unlike neutron scattering, cannot probe away from the zone center.

Figure 3b shows the normalized emission spectra measured for increasing excitation fluence at room temperature. The LE mode is resolved at low excitation densities (0.5−2.5 μJ cm^{-2}), yet it vanishes as the excitation fluence is above 10 μJ cm^{-2}. Under the same excitation fluence range, the TO and HE mode positions and strength remain unaffected. This observation indicates that the microscopic origin of the LE mode is different than those of the two other higher energy modes. We hypothesize that the LE mode is related to correlated local structural fluctuations in PbTe, whose presence was hinted at by prior diffuse scattering measurements on single crystals,[12] as attributed to the ferroelectric-paraelectric structural instability in PbTe.[12] This hypothesis is linked with a prior report of a waterfall-like dispersion of the zone-center TO phonon in PbTe for frequencies below 1 THz.[7] Similar anomalous phonon dispersions have been observed in relaxor-type ferroelectrics due the existence of nanopolar domains[10] and in rattler-type thermoelectrics due to loosely bound rattling dopant atoms.[44] Therefore, the LE mode may stem from localized atomic vibrations associated with correlated local dipolar displacements. Such localized phonon modes have also been predicted in PbTe by first-principles calculations at frequencies below the bare TO mode.[16] Furthermore, disappearance of the LE mode at increased photoexcitation density is also consistent with its origin arising from a structural instability of PbTe. Prior reports showed that increased electronic and photoinduced doping in PbTe suppresses the Peierls-like structural instability and strengthens its paraelectric state[13] and also lowers the Curie temperature.[45] Therefore, the disappearance of the LE mode under increased excitation density may arise due to the suppression of the atomic motion that underlies the structural instability, hence, diminishing correlated local fluctuations. Other possibilities concerning the origin of the LE mode are the existence of extrinsic or intrinsic defects, as well as surface-related effects.[2,21,46] Despite its unclear origin, the photocarrier-dependent response of the LE mode presents opportunities for THz photonic applications. For example, reversible control of the LE phonon mode can be used to make ultrafast (subpicosecond) THz modulators and switches by tuning of the dielectric response in the low energy THz window, 0.1−0.5 THz.

We also study the temperature dependence of the LE, TO, and HE modes as a function of temperature measured at two different excitation fluences (Figure 3c,d). In both fluence cases, the TO mode softens (down to 0.6 THz) and becomes sharper as the temperature decreases from 300 to 80 K. This behavior is consistent with the soft phonon nature of the TO mode, as reported by early works.[2] In the case of the HE mode, decreasing the temperature results in weakening in its strength, yet no significant spectral shift (Figure 3d). This observation contradicts with prior attribution of the double peak structure, that is, TO and HE modes, as arising from strong anharmonic renormalization of the bare TO mode.[17,18,20] Differing temperature-dependent spectral behavior of the TO and HE

https://doi.org/10.1021/acsphotonics.1c01291
ACS Photonics XXXX, XXX, XXX−XXX

modes, for example, softening of the TO mode versus nonshifting of the HE mode, hints about their different microscopic origins. Weakening of the amplitude of the HE mode, which does not spectrally shift much with lowered temperature, may arise due to a strongly anharmonic mode that involves either three or four phonon coupling processes. A similar anomalous response has been observed in CuCl.[47] While the bare TO mode in CuCl showed strong pressure dependence, the three phonon coupled anharmonic mode showed a much lower sensitivity to the pressure, as attributed to weaker sensitivity of the LA + TA modes.[47] Anharmonic interactions have been considered theoretically in PbTe to explain the double peak feature before,[17,18,20] yet it is important to note that our experimental observation does not agree with these prior theoretical works. These reports predicted that the mode at 1.5 THz should soften as the temperature is reduced, while the mode at 1 THz should not, where the experiment shows the reverse happens. The potential explanation for the microscopic origin of the HE mode is the correlated local dipole formation via Pb off-centering in PbTe.[8,12] For the case of the temperature-dependent behavior of the LE mode, we observe that increased excitation fluence suppresses it even at lower temperatures, in agreement with what is observed at room temperature. Under low excitation density, the LE mode slightly softens as the temperature is decreased from 300 to 80 K (Figure 3d). However, another peak-like feature grows in next to the LE mode for temperatures under 150 K. Overall, these results suggest that the physical origins of the TO-like phonons in PbTe are still an open question, yet with clear potential toward THz applications.

CONCLUSION

PbTe has been long considered as a promising material for thermoelectrics and infrared optoelectronics, yet its THz range functionalities arising from anomalous vibrational properties and strong carrier−phonon coupling have not been well understood. Here, we show two key functionalities of PbTe for THz applications: First, we observe a photocarrier density dependent tunable phonon response, enabling spectrally tunable THz emission. We show an unprecedented spectral tunability of the THz emission in the 3.2−2.4 THz range. Second, we uncover a low energy mode at 0.3 THz, which is directly sensitive to the photocarrier density and can be reversibly suppressed under increased excitation density, hence, enabling an all-optical modulation of the THz transmission for applications. Overall, PbTe with large LO−TO splitting, large bandwidth Reststrahlen response, large dielectric coefficients, and photocarrier plasma-coupled tunable ENZ responses stands out as a highly encouraging THz material for practical applications.

METHODS

THz Reflectivity Measurements. We use 1 mm thick ⟨110⟩ ZnTe crystals for both emission and detection of the THz radiation. The 80 nJ pulses from a long cavity Ti:sapphire oscillator (Femtosource XL) at a center wavelength of 798 nm (full-width at half-maximum is 35 nm, pulse width is 45 fs, and repetition rate is 5.12 MHz) are used to excite the ZnTe crystal (spot size is 500 μm). The pump beam is chopped at 320 kHz using an acousto-optic modulator for the lock-in detection. The bandwidth of the system is 2.5 THz. Generated THz field gets reflected from the PbTe surface (total sample area ∼1 cm^2, and sample thickness is 2.5 mm) at an incidence angle of ∼55° and collimated and refocused into the detection crystal by a pair of off-axis parabolic mirrors. The transmitted pump beam through the generation crystal is blocked before reaching PbTe. Generation, reflection, and detection of THz are all performed in a nitrogen-filled box with a relative humidity of zero. As a reference reflector, a thin metal mirror is used at the same position as the sample. Reflected spectrum from the PbTe is compared to that from the metal mirror.

THz Emission Measurements. The setup is schematically depicted in Figure 1a, which is similar to our previous work.[48] We use the same laser system mentioned in the THz reflectivity measurements above. The pump beam is chopped at 320 kHz using an acousto-optic modulator for the lock-in detection. We excite the samples at an incident angle of 55° with respect to the surface normal. The pump spot size on the sample is ∼60 μm. The reflected pump beam is blocked by a thin undoped silicon after the sample before the detection crystal. Pump intensity could be adjusted by a pair of half waveplate and polarizing beam splitter. As an electro-optic detection crystal, we use a 0.25 mm thick ⟨110⟩ GaP giving a detection bandwidth of 8 THz.[49] For Figure 3, 1 mm thick ⟨110⟩ ZnTe crystal was used, which gives a 2.5 THz bandwidth.

Short-Time Fourier Transform Analysis. We use the STFT package provided by OriginPro 2018. Window lengths larger than 2.5 ps consistently reproduce the observed dynamics. When the window length is shorter than 2 ps, dynamics of the small energy modes (<0.5 THz) cannot be accurately resolved. Here, we set the window length to be 3.50 ps and the overlap size to be 3.48 ps. The observed temporal dynamics are independent of the chosen window type. We consistently observe the same results using different types (e.g., Welch, Triangular, Bartlett, Hanning, Hamming, Blackman, etc.). Here, we set the window type to be Hanning. The FFT length is set to 1024.

ASSOCIATED CONTENT

Supporting Information

The Supporting Information is available free of charge at https://pubs.acs.org/doi/10.1021/acsphotonics.1c01291.

Emitter THz polarization state measurement, THz emission under different sample azimuthal orientations, THz emission under different excitation pump polarizations, complex THz dielectric function of PbTe, phonon−plasma coupled mode under varying plasma damping, THz emission temporal profile under low and high excitation density, and THz emission spectra emitted by SnSe under a varying excitation fluence (PDF)

AUTHOR INFORMATION

Corresponding Authors

Burak Guzelturk − *Stanford Institute for Materials and Energy Sciences, SLAC National Accelerator Laboratory, Menlo Park, California 94025, United States; Department of Materials Science and Engineering, Stanford University, Stanford, California 94305, United States; X-ray Science Division, Argonne National Laboratory, Lemont, Illinois 60439, United States;* orcid.org/0000-0003-1977-6485; Email: burakg@anl.gov

https://doi.org/10.1021/acsphotonics.1c01291
ACS Photonics XXXX, XXX, XXX−XXX

Aaron M. Lindenberg − *Stanford Institute for Materials and Energy Sciences, SLAC National Accelerator Laboratory, Menlo Park, California 94025, United States; Department of Materials Science and Engineering, Stanford University, Stanford, California 94305, United States; SLAC National Accelerator Laboratory, Stanford PULSE Institute, Menlo Park, California 94025, United States; Department of Photon Science, Stanford University and SLAC National Accelerator Laboratory, Menlo Park, California 94025, United States;* orcid.org/0000-0003-3233-7161; Email: aaronl@stanford.edu

Authors

Mariano Trigo − *Stanford Institute for Materials and Energy Sciences, SLAC National Accelerator Laboratory, Menlo Park, California 94025, United States; SLAC National Accelerator Laboratory, Stanford PULSE Institute, Menlo Park, California 94025, United States*

Olivier Delaire − *Department of Mechanical Engineering and Materials Science, Duke University, Durham, North Carolina 27708, United States; Department of Physics, Duke University, Durham, North Carolina 27708, United States*

David A. Reis − *Stanford Institute for Materials and Energy Sciences, SLAC National Accelerator Laboratory, Menlo Park, California 94025, United States; SLAC National Accelerator Laboratory, Stanford PULSE Institute, Menlo Park, California 94025, United States; Department of Applied Physics, Stanford University, Stanford, California 94305, United States; Department of Photon Science, Stanford University and SLAC National Accelerator Laboratory, Menlo Park, California 94025, United States*

Complete contact information is available at: https://pubs.acs.org/10.1021/acsphotonics.1c01291

Notes

The authors declare no competing financial interest.

■ ACKNOWLEDGMENTS

This work is supported by the Department of Energy, Office of Science, Basic Energy Sciences, Materials Sciences and Engineering Division, under Contract DE-AC02-76SF00515.

■ REFERENCES

(1) Kanai, Y.; Shohno, K. Dielectric Constant of PbTe. *Jpn. J. Appl. Phys.* **1963**, *2*, 6−10.
(2) Cochran, W.; Cowley, R. A.; Dolling, G.; Elcombe, M. M. The Crystal Dynamics of Lead Telluride. *Proc. R. Soc. A Math. Phys. Eng. Sci.* **1966**, *293*, 433−451.
(3) Xiao, Y.; Zhao, L.-D. Charge and Phonon Transport in PbTe-Based Thermoelectric Materials. *npj Quantum Mater.* **2018**, *3*, 55.
(4) Bilz, H.; Bussmann-Holder, A.; Jantsch, W.; Vogl, P. *Dynamical Properties of IV-VI Compounds; Springer Tracts in Modern Physics*; Springer Berlin Heidelberg: Berlin, Heidelberg, 1983; Vol. *99*.
(5) Heremans, J. P.; Jovovic, V.; Toberer, E. S.; Saramat, A.; Kurosaki, K.; Charoenphakdee, A.; Yamanaka, S.; Snyder, G. J. Enhancement of Thermoelectric Efficiency in PbTe by Distortion of the Electronic Density of States. *Science* **2008**, *321*, 554−557.
(6) Alperin, H. A.; Pickart, S. J.; Rhyne, J. J.; Minkiewicz, V. J. Softening of the Transverse-Optic Mode in PbTe. *Phys. Lett. A* **1972**, *40*, 295−296.
(7) Delaire, O.; Ma, J.; Marty, K.; May, A. F.; McGuire, M. A.; Du, M.-H.; Singh, D. J.; Podlesnyak, A.; Ehlers, G.; Lumsden, M. D.; Sales, B. C. Giant Anharmonic Phonon Scattering in PbTe. *Nat. Mater.* **2011**, *10*, 614−619.
(8) Božin, E. S.; Malliakas, C. D.; Souvatzis, P.; Proffen, T.; Spaldin, N. A.; Kanatzidis, M. G.; Billinge, S. J. L. Entropically Stabilized Local Dipole Formation in Lead Chalcogenides. *Science* **2010**, *330*, 1660−1663.
(9) Jensen, K. M. Ø.; Božin, E. S.; Malliakas, C. D.; Stone, M. B.; Lumsden, M. D.; Kanatzidis, M. G.; Shapiro, S. M.; Billinge, S. J. L. Lattice Dynamics Reveals a Local Symmetry Breaking in the Emergent Dipole Phase of PbTe. *Phys. Rev. B: Condens. Matter Mater. Phys.* **2012**, *86*, 085313.
(10) Gehring, P. M.; Park, S.-E.; Shirane, G. Soft Phonon Anomalies in the Relaxor Ferroelectric Pb (Zn 1/3 Nb 2/3) 0.92 Ti 0.08 O 3. *Phys. Rev. Lett.* **2000**, *84*, 5216−5219.
(11) Manley, M. E.; Lynn, J. W.; Abernathy, D. L.; Specht, E. D.; Delaire, O.; Bishop, A. R.; Sahul, R.; Budai, J. D. Phonon Localization Drives Polar Nanoregions in a Relaxor Ferroelectric. *Nat. Commun.* **2014**, *5*, 3683.
(12) Sangiorgio, B.; Bozin, E. S.; Malliakas, C. D.; Fechner, M.; Simonov, A.; Kanatzidis, M. G.; Billinge, S. J. L.; Spaldin, N. A.; Weber, T. Correlated Local Dipoles in PbTe. *Phys. Rev. Mater.* **2018**, *2*, 085402.
(13) Jiang, M. P.; Trigo, M.; Savić, I.; Fahy, S.; Murray, É. D.; Bray, C.; Clark, J.; Henighan, T.; Kozina, M.; Chollet, M.; Glownia, J. M.; Hoffmann, M. C.; Zhu, D.; Delaire, O.; May, A. F.; Sales, B. C.; Lindenberg, A. M.; Zalden, P.; Sato, T.; et al. The Origin of Incipient Ferroelectricity in Lead Telluride. *Nat. Commun.* **2016**, *7*, 12291.
(14) Lee, S.; Esfarjani, K.; Luo, T.; Zhou, J.; Tian, Z.; Chen, G. Resonant Bonding Leads to Low Lattice Thermal Conductivity. *Nat. Commun.* **2014**, *5*, 3525.
(15) Shiga, T.; Shiomi, J.; Ma, J.; Delaire, O.; Radzynski, T.; Lusakowski, A.; Esfarjani, K.; Chen, G. Microscopic Mechanism of Low Thermal Conductivity in Lead Telluride. *Phys. Rev. B: Condens. Matter Mater. Phys.* **2012**, *85*, 155203.
(16) Zhang, Y.; Ke, X.; Kent, P. R. C.; Yang, J.; Chen, C. Anomalous Lattice Dynamics near the Ferroelectric Instability in PbTe. *Phys. Rev. Lett.* **2011**, *107*, 175503.
(17) Chen, Y.; Ai, X.; Marianetti, C. A. First-Principles Approach to Nonlinear Lattice Dynamics: Anomalous Spectra in PbTe. *Phys. Rev. Lett.* **2014**, *113*, 105501.
(18) Li, C. W.; Hellman, O.; Ma, J.; May, A. F.; Cao, H. B.; Chen, X.; Christianson, A. D.; Ehlers, G.; Singh, D. J.; Sales, B. C.; Delaire, O. Phonon Self-Energy and Origin of Anomalous Neutron Scattering Spectra in SnTe and PbTe Thermoelectrics. *Phys. Rev. Lett.* **2014**, *112*, 175501.
(19) Romero, A. H.; Gross, E. K. U.; Verstraete, M. J.; Hellman, O. Thermal Conductivity in PbTe from First Principles. *Phys. Rev. B: Condens. Matter Mater. Phys.* **2015**, *91*, 214310.
(20) Shiga, T.; Murakami, T.; Hori, T.; Delaire, O.; Shiomi, J. Origin of Anomalous Anharmonic Lattice Dynamics of Lead Telluride. *Appl. Phys. Express* **2014**, *7*, 041801.
(21) Burkhard, H.; Bauer, G.; Lopez-Otero, A. Far-Infrared Reflectivity of PbTe Films on NaCl Substrates. *Solid State Commun.* **1976**, *18*, 773−776.
(22) Wuttig, M.; Deringer, V. L.; Gonze, X.; Bichara, C.; Raty, J.-Y. Incipient Metals: Functional Materials with a Unique Bonding Mechanism. *Adv. Mater.* **2018**, *30*, 1803777.
(23) Yu, P. Y.; Cardona, M. *Fundamentals of Semiconductors; Graduate Texts in Physics*; Springer Berlin Heidelberg: Berlin, Heidelberg, 2010.
(24) Burkhard, H.; Bauer, G.; Lopez-Otero, A. Submillimeter Spectroscopy of TO-Phonon Mode Softening in PbTe. *J. Opt. Soc. Am.* **1977**, *67*, 943.
(25) Tani, M.; Fukasawa, R.; Abe, H.; Matsuura, S.; Sakai, K.; Nakashima, S. Terahertz Radiation from Coherent Phonons Excited in Semiconductors. *J. Appl. Phys.* **1998**, *83*, 2473−2477.
(26) Gu, P.; Tani, M.; Kono, S.; Sakai, K.; Zhang, X.-C. Study of Terahertz Radiation from InAs and InSb. *J. Appl. Phys.* **2002**, *91*, 5533−5537.
(27) Wu, Q.; Zhang, X.-C. Free-space Electro-optic Sampling of Terahertz Beams. *Appl. Phys. Lett.* **1995**, *67*, 3523−3525.

(28) Guzelturk, B.; Mei, A. B.; Zhang, L.; Tan, L. Z.; Donahue, P.; Singh, A. G.; Schlom, D. G.; Martin, L. W.; Lindenberg, A. M. Light-Induced Currents at Domain Walls in Multiferroic $BiFeO_3$. *Nano Lett.* **2020**, *20*, 145.
(29) Zhang, X.-C.; Hu, B. B.; Darrow, J. T.; Auston, D. H. Generation of Femtosecond Electromagnetic Pulses from Semiconductor Surfaces. *Appl. Phys. Lett.* **1990**, *56*, 1011−1013.
(30) Gu, P.; Tani, M. Terahertz Radiation from Semiconductor Surfaces. In *Terahertz Optoelectronics*; Springer-Verlag: Berlin/Heidelberg, 2005; pp 63−98.
(31) Dekorsy, T.; Auer, H.; Waschke, C.; Bakker, H. J.; Roskos, H. G.; Kurz, H.; Wagner, V.; Grosse, P. Emission of Submillimeter Electromagnetic Waves by Coherent Phonons. *Phys. Rev. Lett.* **1995**, *74*, 738−741.
(32) Tani, M.; Fukasawa, R.; Abe, H.; Matsuura, S.; Sakai, K.; Nakashima, S. Terahertz Radiation from Coherent Phonons Excited in Semiconductors. *J. Appl. Phys.* **1998**, *83*, 2473−2477.
(33) Dekorsy, T.; Cho, G. C.; Kurz, H. Coherent Phonons in Condensed Media. In *Light Scattering in Solids VIII*; Springer Berlin Heidelberg, 2000; pp 169−209.
(34) Dekorsy, T.; Auer, H.; Bakker, H. J.; Roskos, H. G.; Kurz, H. THz Electromagnetic Emission by Coherent Infrared-Active Phonons. *Phys. Rev. B: Condens. Matter Mater. Phys.* **1996**, *53*, 4005−4014.
(35) Caldwell, J. D.; Lindsay, L.; Giannini, V.; Vurgaftman, I.; Reinecke, T. L.; Maier, S. A.; Glembocki, O. J. Low-Loss, Infrared and Terahertz Nanophotonics Using Surface Phonon Polaritons. *Nanophotonics* **2015**, *4*, 44−68.
(36) Shan, J.; Heinz, T. F. Terahertz Radiation from Semiconductors. In *Ultrafast Dynamical Processes in Semiconductors; Topics in Applied Physics*; Tsen, K., Ed.; Springer Berlin Heidelberg, 2004; Vol *92*, pp 1−56.
(37) Varga, B. B. Coupling of Plasmons to Polar Phonons in Degenerate Semiconductors. *Phys. Rev.* **1965**, *137*, A1896−A1902.
(38) Basak, A. K.; Petek, H.; Ishioka, K.; Thatcher, E. M.; Stanton, C. J. Ultrafast Coupling of Coherent Phonons with a Nonequilibrium Electron-Hole Plasma in GaAs. *Phys. Rev. B: Condens. Matter Mater. Phys.* **2015**, *91*, 125201.
(39) Dreyer, C. E.; Coh, S.; Stengel, M. Nonadiabatic Born Effective Charges in Metals and the Drude Weight. *arXiv:2103.04425 [cond-mat.mtrl-sci]* **2021**, na.
(40) Reklaitis, A. Terahertz Emission from InAs Induced by Photo-Dember Effect: Hydrodynamic Analysis and Monte Carlo Simulations. *J. Appl. Phys.* **2010**, *108*, 053102.
(41) Reid, M.; Cravetchi, I. V.; Fedosejevs, R. Terahertz Radiation and Second-Harmonic Generation from InAs: Bulk versus Surface Electric-Field-Induced Contributions. *Phys. Rev. B: Condens. Matter Mater. Phys.* **2005**, *72*, 035201.
(42) Yang, Y.; Kamaraju, N.; Campione, S.; Liu, S.; Reno, J. L.; Sinclair, M. B.; Prasankumar, R. P.; Brener, I. Transient GaAs Plasmonic Metasurfaces at Terahertz Frequencies. *ACS Photonics* **2017**, *4*, 15−21.
(43) Jia, W.; Liu, M.; Lu, Y.; Feng, X.; Wang, Q.; Zhang, X.; Ni, Y.; Hu, F.; Gong, M.; Xu, X.; Huang, Y.; Zhang, W.; Yang, Y.; Han, J. Broadband Terahertz Wave Generation from an Epsilon-near-Zero Material. *Light: Sci. Appl.* **2021**, *10*, 11.
(44) Cohn, J. L.; Nolas, G. S.; Fessatidis, V.; Metcalf, T. H.; Slack, G. A. Glasslike Heat Conduction in High-Mobility Crystalline Semiconductors. *Phys. Rev. Lett.* **1999**, *82*, 779−782.
(45) Kobayashi, K. L. I.; Kato, Y.; Katayama, Y.; Komatsubara, K. F. Carrier-Concentration-Dependent Phase Transition in SnTe. *Phys. Rev. Lett.* **1976**, *37*, 772−774.
(46) Sun, Y.; Zhou, Y.; Han, J.; Liu, W.; Nan, C.; Lin, Y.; Hu, M.; Xu, B. Strong Phonon Localization in PbTe with Dislocations and Large Deviation to Matthiessen's Rule. *npj Comput. Mater.* **2019**, *5*, 97.
(47) Ulrich, C.; Göbel, A.; Syassen, K.; Cardona, M. Pressure-Induced Disappearance of the Raman Anomaly in CuCl. *Phys. Rev. Lett.* **1999**, *82*, 351−354.
(48) Guzelturk, B.; Belisle, R. A.; Smith, M. D.; Bruening, K.; Prasanna, R.; Yuan, Y.; Gopalan, V.; Tassone, C. J.; Karunadasa, H. I.; McGehee, M. D.; Lindenberg, A. M. Terahertz Emission from Hybrid Perovskites Driven by Ultrafast Charge Separation and Strong Electron-Phonon Coupling. *Adv. Mater.* **2018**, *30*, 1704737.
(49) Ma, E. Y. E. Y.; Guzelturk, B.; Li, G.; Cao, L.; Shen, Z.-X. Z.-X.; Lindenberg, A. M. A. M.; Heinz, T. F. T. F. Recording Interfacial Currents on the Subnanometer Length and Femtosecond Time Scale by Terahertz Emission. *Sci. Adv.* **2019**, *5*, eaau0073.

https://doi.org/10.1021/acsphotonics.1c01291
ACS Photonics XXXX, XXX, XXX−XXX